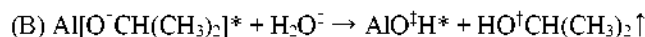
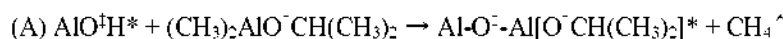


Preparation of Al₂O₃ Thin Films by Atomic Layer Deposition Using Dimethylaluminum Isopropoxide and Water and Their Reaction Mechanisms

Ki-Seok An, Wontae Cho, Kiwhan Sung, Sun Sook Lee, and Yunsoo Kim*

*Thin Film Materials Laboratory, Advanced Materials Division,
Korea Research Institute of Chemical Technology, Yuseong P.O. Box 107, Daejeon 305-600, Korea
Received July 1, 2003*

Al₂O₃ thin films were grown on H-terminated Si(001) substrates using dimethylaluminum isopropoxide [DMAI: (CH₃)₂AlOCH(CH₃)₂], as a new Al precursor, and water by atomic layer deposition (ALD). The self-limiting ALD process by alternate surface reactions of DMAI and H₂O was confirmed from measured thicknesses of the aluminum oxide films as functions of the DMAI pulse time and the number of DMAI-H₂O cycles. Under optimal reaction conditions, a growth rate of ~1.06 Å per ALD cycle was achieved at the substrate temperature of 150 °C. From a mass spectrometric study of the DMAI-D₂O ALD process, it was determined that the overall binary reaction for the deposition of Al₂O₃ [2 (CH₃)₂AlOCH(CH₃)₂ + 3 H₂O → Al₂O₃ + 4 CH₄ + 2 HOCH(CH₃)₂] can be separated into the following two half-reactions:



where the asterisks designate the surface species. Growth of stoichiometric Al₂O₃ thin films with carbon incorporation less than 1.5 atomic % was confirmed by depth profiling Auger electron spectroscopy. Atomic force microscopy images show atomically flat and uniform surfaces. X-ray photoelectron spectroscopy and cross-sectional high resolution transmission electron microscopy of an Al₂O₃ film indicate that there is no distinguishable interfacial Si oxide layer except that a very thin layer of aluminum silicate may have been formed between the Al₂O₃ film and the Si substrate. *C-V* measurements of an Al₂O₃ film showed capacitance values comparable to previously reported values.

Key Words : Aluminum oxide, Atomic layer deposition (ALD), Dimethylaluminum isopropoxide, Surface chemical reaction

Introduction

Atomic layer deposition (ALD) is a deposition technique for growing high-quality thin films based on alternate self-limiting surface chemical reactions. ALD has some advantages over other techniques such as good uniformity, controllability of thickness due to the self-limiting property, better step coverage, good stoichiometry due to functional reactions, and relatively low deposition temperature. ALD technique has been rapidly adopted in microelectronic device processes to deposit a wide variety of thin film materials such as oxides, nitrides, and metals.^{1,2}

Al₂O₃ is probably one of the most extensively studied materials by ALD. It is an attractive dielectric material due to its large band gap (~9 eV) and large band offsets with respect to Si. Its thermal and chemical stability allows its application as a good diffusion barrier material.^{3,4} Several precursors such as AlCl₃, Me₂AlCl, Me₃Al, Et₃Al, Al(OEt)₃, and Al(OⁱPr)₃ have been adopted with oxygen sources such as O₂, H₂O, and O₃ for the growth of Al₂O₃ thin films of high quality in both ALD and chemical vapor deposition (CVD) processes.^{1,2} Recently, aluminum alkoxides as oxygen

source, instead of H₂O, etc., were combined with AlCl₃ to avoid formation of an undesired interfacial SiO₂ layer.^{5,6} In order to successfully obtain high quality films in ALD processes and apply them to the preparation of microelectronic devices, the choice of suitable precursors is essentially important. Among the precursors, trimethylaluminum (Me₃Al, TMA) has been extensively used because of its high volatility and thermal stability, and the chemical reaction mechanism in the TMA-H₂O ALD process has been well established.^{1,2,7}

In this study, the growth of Al₂O₃ thin films using dimethylaluminum isopropoxide [DMAI: (CH₃)₂AlOCH(CH₃)₂], as a new Al precursor, and water by ALD and their surface chemical reactions have been investigated. DMAI, a liquid at room temperature, has a reasonably high vapor pressure for ALD and MOCVD,^{8,9} contains no halogens and is not pyrophoric. This study concentrated on the confirmation of the usefulness of the DMAI precursor, its ALD mechanism, and identification of the interfacial oxidation states of the silicon substrates.

Experimental Section

A commercial ALD reactor (Genitech, Inc., prototype)

*Corresponding author. e-mail: yunsukim@kriict.re.kr

was used to grow the Al_2O_3 films. Argon was used as a carrier and purge gas. The Si substrates were first cleaned in a 4% HF solution to remove native oxide layers and prepare H-terminated surfaces. They were then rinsed with deionized water and blown free of particles with dry nitrogen before loading into the ALD reactor.

One ALD cycle (AB cycle) was performed using the following sequence: A (DMAI: 0.1-1 s) - Ar purge (2 s) - B (H_2O : 0.5 s) - Ar purge (2 s). A self-limiting ALD process was checked with thickness measurements of the grown films against the precursor pulse time and the number of AB cycles. During the ALD process, the DMAI precursor and the substrate were kept at 85 °C and 150 °C, respectively. After certain numbers of AB reaction cycles were completed, the thickness of the film deposited was measured by ellipsometry (Gaertner, L116B) using a He-Ne laser in air. The Al_2O_3 films were characterized by Auger electron spectroscopy (AES), atomic force microscopy (AFM), and transmission electron microscopy (TEM).

In addition, in order to clarify the surface chemical reactions in the ALD process, the gas compositions immediately after the DMAI- D_2O reaction were measured in a differentially pumped quadrupole mass analyzer (QMA) chamber directly connected to the ALD reactor using a bypass line. The films were further characterized by AES depth profiling, X-ray photoelectron spectroscopy (XPS), cross-sectional high resolution transmission electron microscopy (HRTEM), and $C-V$ measurements.

Results and Discussion

The optimized self-limiting ALD process and reaction mechanism. The optimized self-limiting ALD process was confirmed by the measurements of film thickness against the DMAI pulse time and the number of DMAI- H_2O ALD cycles. Figure 1 shows the film thickness versus the DMAI pulse time (for Al_2O_3 films deposited with 200 ALD cycles) and the number of DMAI- H_2O ALD cycles with the DMAI pulse time of 0.5 s, denoted by triangles and circles, respectively. The film thickness increases rapidly with the

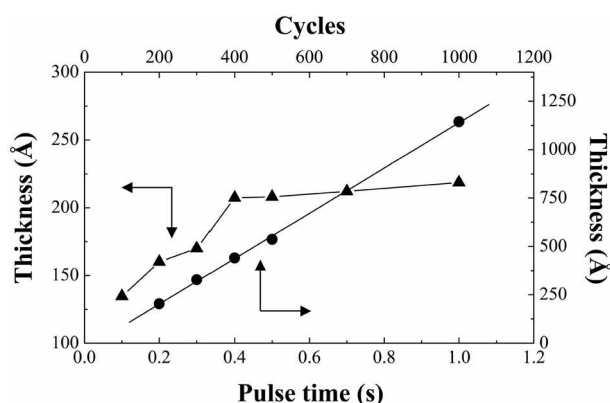


Figure 1. Thickness as functions of DMAI pulse time (with 200 AB cycles, \blacktriangle) and the number of AB (\bullet) cycles for the Al_2O_3 films deposited on H-terminated Si(001) substrates at 150 °C.

DMAI pulse time and is almost constant when the pulse time is longer than 0.4 s. This behavior indicates that the optimized self-limiting ALD reaction is reached at the pulse time over 0.4 s. In an optimized self-limiting ALD process, a constant growth rate per AB cycle is achieved without additional film growth for prolonged source exposures. The constant growth rate implies that the self-limiting ALD process is proper without a CVD effect at a suitable substrate temperature. As shown in Figure 1, the Al_2O_3 film thickness is directly proportional to the number of AB cycles. From the thickness measurements, the Al_2O_3 growth rate of DMAI- H_2O ALD process under optimized conditions is $\sim 1.06 \text{ \AA/AB cycle}$. The growth rate of the DMAI- H_2O ALD process is comparable to that of a typical TMA- H_2O ALD process at similar deposition temperatures.¹⁰⁻¹²

In order to elucidate the chemical reactions in the DMAI- H_2O ALD process, the reaction products after each of the cyclic reactions were monitored by a differentially pumped QMA, which was connected to the outlet side of the reactor. D_2O was used, instead of H_2O , to distinguish the expected reaction products $\{\text{CH}_4$ and $\text{OCH}_2(\text{CH}_3)_2\}$ in the DMAI- H_2O ALD process from the fragments directly formed by the decomposition of DMAI. To examine the reactions, the following pulsing sequence was used: 4 times 0.5 s DMAI pulse 4 times (successive 0.5 s D_2O - 0.5 s DMAI pulses) - 5 times 0.5 s D_2O pulse. To minimize formation of undesired chemical reactions caused by residual gases in the reactor, a long pumping sequence of 500 s was performed after each DMAI pulse.

Figure 2 shows the behavior of important selected masses during the DMAI- D_2O ALD process at the substrate temperature of 150 °C. DMAI ($m/z = 116$), D_2O ($m/z = 20$), and the expected main reaction products, CH_3D ($m/z = 17$) and $\text{CH}(\text{CH}_3)_2\text{OD}$ ($m/z = 61$), were monitored during the ALD cycles.

First, when only DMAI was pulsed, the signal $m/z = 116$ behaved consistently with respect to the sequence. On the other hand, when DMAI was pulsed right after a D_2O pulse, its signal intensity decreased substantially. This behavior must have resulted from the decrease in the number of

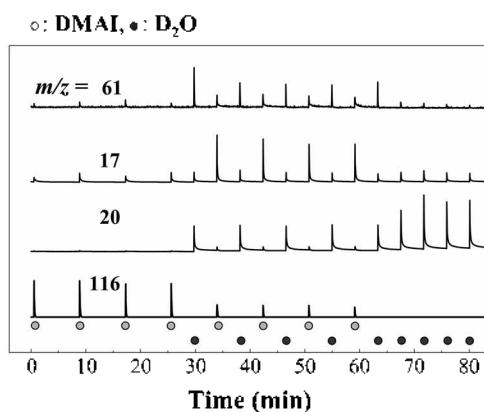
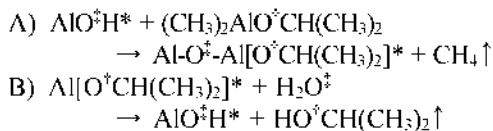


Figure 2. Intensities of selected masses in the DMAI- D_2O ALD process at the substrate temperature of 150 °C as a function of pulse sequence.

DMAI molecules due to the chemical reaction on the OD-terminated surface formed by the D₂O pulse. Similar behavior in the signal $m/z = 20$ was observed when only D₂O was pulsed. The signal $m/z = 20$ increased at the successive final four D₂O pulses.

Small signals of $m/z = 17, 61,$ and 20 were observed at the first four DMAI pulses, which may have been caused by the limited mass resolution and/or imperfect pumping of the residual gases in the reactor. Actually, the signals $m/z = 16$ (CH₄) and 60 [CH(CH₃)₂OH] were detected when DMAI alone was pulsed. The presence of neighboring peaks could increase the signals $m/z = 17$ and 61 . And partial chemical reaction between DMAI and the residual D₂O remaining in the reactor due to imperfect pumping can not be excluded. Similar explanation for the signals $m/z = 17$ and 61 for the final four D₂O pulses may be possible.

Next, for the alternate DMAI-D₂O pulses, the signal $m/z = 61$ increased significantly during the D₂O pulses and decreased during the DMAI pulses. On the other hand, the signal $m/z = 17$ showed the opposite behavior. This indicates that the main chemical interactions on DMAI-exposed and D₂O-exposed surfaces are different. The Al-OCH(CH₃)₂* surface is formed on the top layer during a DMAI pulse and CH(CH₃)₂OD is mainly produced from the surface during a D₂O pulse. The Al-OD* surface is formed during a D₂O pulse and CH₃D is mainly produced during a DMAI pulse due to the reaction between the Al-OD* surface and the methyl groups of the DMAI precursor. From these results, the DMAI-H₂O half-reactions may be described by the following alternate half-reactions:



and the overall AB binary reaction is:

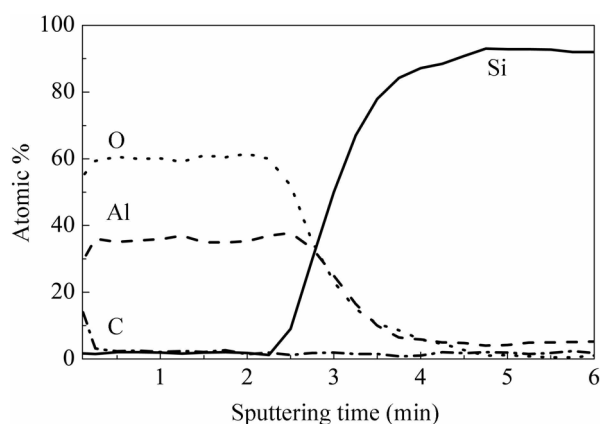
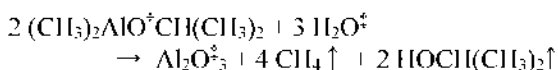


Figure 3. AES depth profile of an Al₂O₃ film on H-terminated Si(001) grown with 400 AB cycles at the substrate temperature of 150 °C.

where the asterisks denote the surface species. However, a reverse reaction may not be completely excluded because a small signal for CH(CH₃)₂OD was apparently observed during the DMAI pulse.

It is interesting to note a previous Fourier transform infrared (FTIR) spectroscopic investigation of the DMAI precursor carried out at various CVD reactor temperatures.⁹ In the IR spectra, all bands induced by the DMAI precursor were consistently observed in the reactor temperature up to 500 °C. The band intensities started to decrease above 540 °C and completely disappeared at 580 °C. This result is indicative of the stability of the DMAI precursor without any thermal decomposition up to ~500 °C. Comparing the FTIR measurements with our QMA results of Figure 2, it is found that the presence of H₂O greatly favors the precursor decomposition process.

Characterization of Al₂O₃ thin films and the interfaces.

The stoichiometry and contamination of aluminum oxide thin films were investigated by AES depth profile. Figure 3 shows the AES depth profiling result of a film grown with 400 AB cycles at 150 °C. The ratio of Al : O was measured to be 2.0 : 3.2 with the carbon incorporation less than 1.5% throughout the depth of the film except at the top surface region. The low carbon incorporation implies that the methyl and isopropoxide groups of DMAI are almost completely removed by the binary reactions.

Surface roughness of the Al₂O₃ films was measured by AFM. Figure 4 shows the AFM images for the Al₂O₃ films

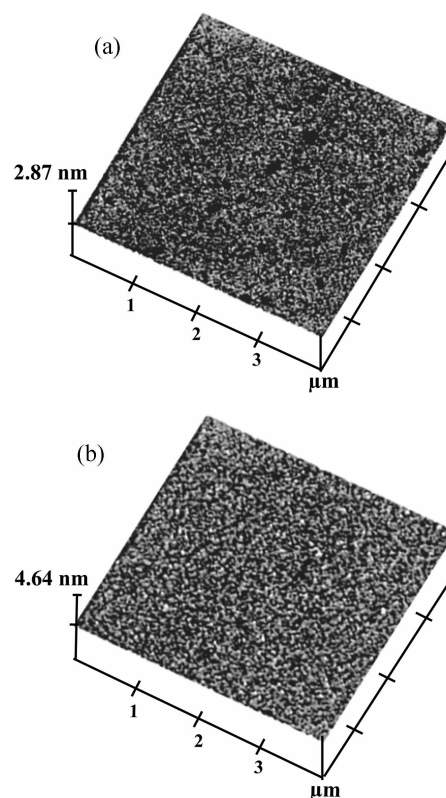


Figure 4. Atomic force microscopy images of Al₂O₃ films deposited at 150 °C on H-terminated Si(001) substrates with 20 AB cycles (a) and 250 AB cycles (b).

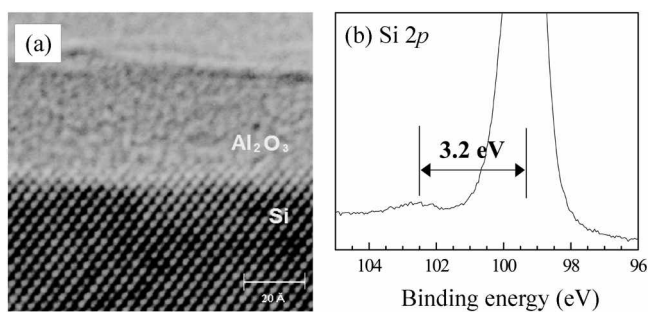


Figure 5. A cross-sectional HRTEM image of an interface between a 3.5 nm-thick Al_2O_3 film and the Si(001) substrate (a) and the Si 2p core level XP spectrum (b).

grown with 20 (a) and 250 (b) AB cycles. The AFM images reveal extremely flat and uniform surfaces. The root-mean-square (RMS) roughness values are 1.17 Å and 1.70 Å, respectively, which are comparable to those of the films obtained by the TMA- H_2O ALD process.¹¹ The uniform and atomic-scale surface roughness of the two films differing very much in thickness clearly indicates that the growth conditions for the Al_2O_3 ALD process have been properly optimized.

Figure 5(a) shows a cross-sectional HRTEM image of the interface between a 35 Å thick Al_2O_3 film and the Si substrate. The image clearly shows that only a monolayer-thick interface imaged a slightly light area at the interface. To investigate the chemical composition of the interfacial layer and see whether it is Si oxide or silicate, the Si 2p core level XP spectrum of the film was taken as shown in Figure 5(b). In this figure, a very small and broad peak appears at the binding energy of ~102.5 eV. The binding energy shift (ΔE) with respect to the bulk Si 2p core level (Si^0) was measured to be ~3.2 eV. The binding energy shift is clearly much larger than the value ($\Delta E = 2.65$ eV) for the Si^{3-} and smaller than the value ($\Delta E = 3.57$ –4 eV) for the Si^{4+} in conventional SiO_2/Si interfaces.^{13,14} Although a detailed discussion of the presence of suboxide components is difficult because of the limited energy resolution and weak intensity, the ΔE value of 3.2 eV in our film may suggest the presence of a silicate component (Si-O-Al). In previous XPS measurements of ultrathin $\text{Al}_2\text{O}_3/\text{Si}$ and $\text{Al}_2\text{O}_3/\text{SiO}_2$ interfaces, the component with the ΔE value of 3.2 eV was properly identified to be the contribution of Si-O-Al bonds in the aluminum silicate layer formed at the interfaces.^{14,15} Combined with the TEM image, our XPS result shows that only a monolayer-thick interfacial silicate layer was formed between the Al_2O_3 film and the Si substrate.

The Al_2O_3 thin films were then investigated by electrical measurements to see if they would be suitable as a prospective capacitor material. A 273 Å-thick Al_2O_3 film deposited at 150 °C was subjected to C - V measurements as-deposited and after rapid thermal annealing (RTA) up to 600 °C. The dielectric constant of the film before RTA was measured to be ~7.7 which is somewhat smaller than the bulk value of Al_2O_3 ($K = 9$ –11). The RTA was performed in a nitrogen atmosphere starting from room temperature to

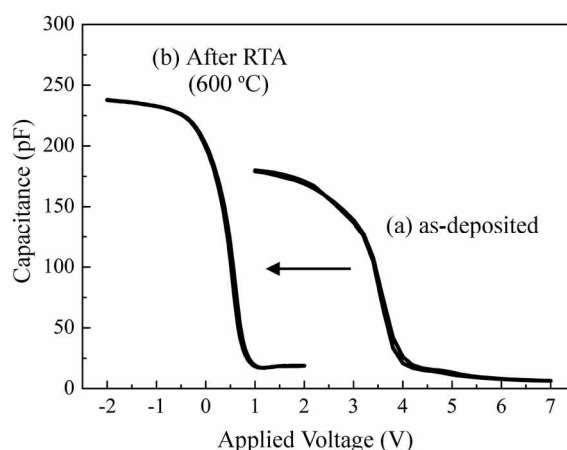


Figure 6. C - V measurements of an Al_2O_3 film as-deposited (a) and after RTA to 600 °C (b).

reach 600 °C in ~20 s, at which the film was held for 40 s and cooled afterward. After the RTA, the film showed a flat band shift of ~3 eV toward the zero voltage with an increase in capacitance. This behavior indicates that the RTA process must have made changes in the interfacial states between the Al_2O_3 film and the Si substrate although the details of the interfacial states are not known at this stage. And the process probably made the film denser by shrinkage resulting in the increase in its capacitance.¹⁶ Due to the increase in capacitance of the film by the RTA process, its dielectric constant increased to ~8.9.

Summary

In this study, Al_2O_3 thin films were grown on H-terminated Si(001) substrates using dimethylaluminum isopropoxide as a new Al precursor and water by atomic layer deposition. The thickness measurements show a well-optimized self-limiting DMAI- H_2O ALD process with a growth rate of ~1.06 Å/AB cycle at the substrate temperature of 150 °C. From mass spectrometric studies for DMAI- D_2O ALD process, the binary reaction separated into two half-reactions is confirmed.

Film characterization by AES depth profile and AFM images shows low carbon incorporation less than 1.5 atomic % in the grown Al_2O_3 thin films and extremely flat and uniform surfaces. XPS and HRTEM results indicate that there is no distinguishable interfacial Si oxide layer except that there is a possibility for existence of a very thin layer of aluminum silicate (Si-O-Al) between the Al_2O_3 film and the Si substrate. Measurements of dielectric constants indicate that the Al_2O_3 films prepared from DMAI and water may be useful as a capacitor material.

Acknowledgments. This research has been supported by the Ministry of Science and Technology of Korea through the National Program for Tera-level Nanodevices (TND) as one of the 21st Century Frontier Programs and the National Research Laboratory (NRL) Program.

References

1. Suntola, T. *Thin Films and Epitaxy* in *Handbook of Crystal Growth*, Hurler, D. T. J., Ed.; Elsevier Science: Amsterdam, 1994; Vol. 3, pp. 601-663 and references therein.
 2. Ritala, M.; Leskelä, M. *Deposition and Processing of Thin Films* in *Handbook of Thin Film Materials*, Nalwa, H. S., Ed.; Academic Press: San Diego, 2002; Vol. 1, pp. 103-159 and references therein.
 3. Wilk, G. D.; Wallace, R. M.; Anthony, J. M. *J. Appl. Phys.* **2001**, *89*, 5243-5275.
 4. Copel, M.; Cartier, E.; Gusev, E. P.; Guha, S.; Bojarczuk, N.; Poppeller, M. *Appl. Phys. Lett.* **2001**, *78*, 2670-2672.
 5. Ritala, M.; Kukli, K.; Rahtu, A.; Räisänen, P. I.; Leskelä, M.; Sajavaara, T.; Keinonen, J. *Science* **2000**, *288*, 319-321.
 6. Räisänen, P. I.; Ritala, M.; Leskelä, M. *J. Mater. Chem.* **2002**, *12*, 1415-1418.
 7. Juppo, M.; Tahtu, A.; Ritala, M.; Leskelä, M. *Langmuir* **2000**, *16*, 4034-4039.
 8. Koh, W.; Ku, S.-J.; Kim, Y. *Thin Solid Films* **1997**, *304*, 222-224.
 9. Barreca, D.; Battiston, G. A.; Gerbasi, R.; Tondello, E. *J. Mater. Chem.* **2000**, *10*, 2127-2130.
 10. Higashi, G. S.; Fleming, C. G. *Appl. Phys. Lett.* **1989**, *55*, 1963-1965.
 11. Ott, A. W.; McCarley, K. C.; Klaus, J. W.; Way, J. D.; George, S. M. *Appl. Surf. Sci.* **1996**, *107*, 128-136.
 12. George, S. M.; Ott, A. W.; Klaus, J. W. *J. Phys. Chem.* **1996**, *100*, 13121-13131.
 13. Green, M. L.; Gusev, E. P.; Degraeve, R.; Garfunkel, E. L. *J. Appl. Phys.* **2001**, *90*, 2057-2121.
 14. Renault, O.; Gosset, L. G.; Rouchon, D.; Ermolief, A. *J. Vac. Sci. Technol. A* **2002**, *20*, 1867-1876.
 15. Klein, T. M.; Niu, D.; Epling, W. S.; Li, W.; Maher, D. M.; Hobbs, C. C.; Hegde, R. I.; Baumvol, I. J. R.; Parsons, G. N. *Appl. Phys. Lett.* **1999**, *75*, 4001-4003.
 16. Jakschik, S.; Schroeder, U.; Hecht, T.; Gutsche, M.; Seidl, H.; Bartha, J. W. *Thin Solid Films* **2003**, *425*, 216-220.
-